

# Investigating the Extracellular Contribution to the Double-Wave-Vector Diffusion-Weighted Signal

Patricia Ulloa<sup>1</sup>, Viktor Wottschel<sup>2</sup>, and Martin A. Koch<sup>1</sup>

<sup>1</sup>Institute of Medical Engineering, University of Lübeck, Lübeck, Germany, <sup>2</sup>Queen Square MS Centre, UCL Institute of Neurology, University College London, London, United Kingdom

**INTRODUCTION** Using two independent periods of diffusion weighting between excitation and acquisition, known as double diffusion encoding or double wave vector (DWV) diffusion weighting, it is possible to acquire information on the pore size and shape in tissue *in vivo* [1], for which no other non-invasive technique exists. This may provide a new tool for tissue characterization applicable to clinical questions. An estimate of the pore size can be derived from the signal difference between parallel and antiparallel diffusion gradient orientations. Recent experiments applied this to the human corticospinal tract (CST) *in vivo* [2]. However, an analysis that assumes cylindrical pores [2,3] yields pore diameters well above the most frequent axon diameter to be expected in the CST. This could be due to the contribution of pores in the extracellular space, which can be considerably wider than the intra-axonal compartment. The study presented here exploits the unique shape sensitivity of the DWV signal to acquire information on extracellular contributions to the DWV pore size results. It is assumed that the intracellular compartment in a fibre tract is most likely to be represented by a right circular cylinder, while the extracellular compartment may be better represented by cylinders with an irregular base (if closed pores are assumed).

**THEORY AND METHODS** In a perpendicular cross section through a densely packed set of circular cylinders of identical radius, the cross sections of the cylinders are circles whereas the space between the cylinders resembles an equilateral triangle with indented edges (Fig 1A and B). For randomly oriented nonspherical pores, overall diffusion is isotropic but the pore eccentricity can still be detected from comparing DWV experiments with parallel and perpendicular diffusion gradients. *In vivo*, the anisotropy of tissue complicates the situation but this can be averaged out [4]. The parallel-perpendicular signal difference should bear information on the shape of the compartments dominating the DWV pore size estimate in the CST, with all diffusion gradients being roughly perpendicular to the fibre axis. The suggested averaging schemes should not be applied here as they aim at measuring the eccentricity of a 3D pore, and long cylindrical pores are always eccentric. Unfortunately, it can be shown in simulations that the extracellular space cross sections shown in Fig. 1B are too symmetric to induce a parallel-perpendicular difference in DWV experiments. However, if the cylinders are different in size and/or are not perfectly densely packed, the extracellular space cross sections can assume irregular shape and random orientation (Fig 1C). This would induce a signal difference between parallel and perpendicular gradient orientations. The intracellular compartment will not exhibit such a sign of pore eccentricity since its cross section is likely to be almost circular.

The parallel-perpendicular signal difference arises from the following reasoning. In a setting of identical eccentric 2D pores where the same number of pores have its long axis along the  $x$  and  $y$  axis, respectively, the signal attenuations  $E = S/S_0$  for parallel and perpendicular gradient orientations are in general not equal,

$$E_{\text{perp}} = \exp(-bD_1) \exp(-bD_2) + \exp(-bD_2) \exp(-bD_1) \neq \exp(-bD_1) \exp(-bD_1) + \exp(-bD_2) \exp(-bD_2) = E_{\text{par}}. \quad \text{Eq. (1)}$$

Here,  $D_1$  and  $D_2$  are the effective diffusion coefficients along the two perpendicular diffusion gradient directions involved, and  $b = \gamma^2 G^2 \delta^2 (\Delta - \delta/3)$ . Equation (1) is the basis for the eccentricity estimation by DWV. It means that a parallel-perpendicular DWV signal difference in the CST experiment can indicate contributions from the extracellular space. In measurements of the CST however, the complication arises that the plane containing the diffusion gradients may be tilted with respect to the fibre axis (Fig 1D). This can also lead to differences between parallel and perpendicular DWV signals. Nevertheless, that difference can be removed by a specific averaging because it is not equal for all gradients in the plane: for a voxel containing only a single orientation of eccentric 2D pores,

$$E_{\text{perp}} = \exp(-bD_1) \exp(-bD_2) \neq \exp(-bD_1) \exp(-bD_1) = E_{\text{par}} \quad \text{Eq. (2)}$$

can occur. Then, rotating all gradients by  $90^\circ$  will yield

$$E_{\text{perp}} = \exp(-bD_2) \exp(-bD_1) \neq \exp(-bD_2) \exp(-bD_2) = E_{\text{par}}. \quad \text{Eq. (3)}$$

After a geometric mean of the signals given in Eqs. (2) and (3) the parallel-perpendicular difference should vanish. This reasoning can be transferred to both elliptic (Fig 1E) and tilted circular cylinders. If the difference remains, more than one orientation of eccentric cylinders must be present as in Eq. (1), or circular cylinders with more than one direction of inclination. Considering the homogeneous structure of the CST, different inclinations in a single voxel are unlikely. It can then be concluded that the space dominating the signal is irregularly shaped. This would point to the extracellular space as the origin of the DWV signal.

DWV experiments were performed on porcine spinal cord (fixed in formalin) and on two healthy volunteers, using SE-EPI with double diffusion encoding with short  $\tau_m$  on a 3 T whole-body MR system (Ingenia, Philips, Amsterdam) using an 8 channel head coil array. For the spinal cord sample, 1 slice with  $1.2 \times 1.2 \times 10 \text{ mm}^3$  nominal resolution was used,  $\delta = 17 \text{ ms}$ ,  $\Delta = 103 \text{ ms}$ , time between start of 2<sup>nd</sup> and 3<sup>rd</sup> diffusion gradient pulse  $\tau_m = \delta + 0.9 \text{ ms}$  and  $TE/TR = 300 \text{ ms} / 4 \text{ s}$ . Four different gradient vectors were acquired, each with 12 gradient directions and 10 repetitions. *In vivo*, 20 transverse slices were acquired with  $3 \times 3 \times 3 \text{ mm}^3$  nominal resolution,  $\delta = 10 \text{ ms}$ ,  $\Delta = 62 \text{ ms}$ ,  $\tau_m = \delta + 0.9 \text{ ms}$ ,  $TE = 180 \text{ ms}$ ,  $TR = 4.4 \text{ s}$  and  $6.5 \text{ s}$ , respectively, 15 repetitions. For the diffusion gradients, parallel, antiparallel, and perpendicular combinations of the four directions with equal  $x$  and  $y$  (and zero  $z$ ) components were used, where  $z$  is along the body axis. The mean squared radius of gyration  $\langle R^2 \rangle$  as an estimate of pore size was calculated *in vivo* for comparison. The spinal cord was approximately aligned with the  $z$  axis. For a region-of-interest (ROI) analysis both left and right CST were delineated manually starting from a thresholded diffusion-weighted image. Separate diffusion tensor imaging was also performed to estimate the fibre directions.

**RESULTS AND DISCUSSION** The geometric mean provided positive parallel-perpendicular signal differences in the ROI covering the CST (Fig 2.). The spinal cord experiments also yielded a positive difference. The findings suggest a significant contribution of a compartment which is eccentric in the plane of the diffusion gradients. This is consistent with the irregularly bounded extracellular compartment being the predominant origin of the measured signal. The mean  $\langle R^2 \rangle$  derived from the antiparallel-parallel signal difference *in vivo* was  $(3.51 \pm 0.07) \mu\text{m}^2$ , which for ellipsoidal pores would mean an average pore diameter  $2r_{av} \approx 4.8 \mu\text{m}$ , in the same order of magnitude as in [2].

**REFERENCES** [1] PP Mitra, *Phys. Rev. B* **51**, 15074 (1995) ; [2] MA Koch, J Finsterbusch, *NMR Biomed.* **24**, 1422 (2011); [3] E Özarslan, PJ Basser, *J. Chem. Phys.* **128**, 154511 (2008); [4] SN Jespersen et al., *NMR Biomed.* **26**, 1647 (2013)

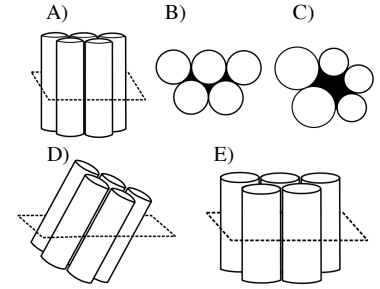


Fig 1. A) Packed circular cylinders. B) cross section of A. C) possible cross sections in a lower density packing. D) Tilted cylinders. E) Elliptical cylinders.

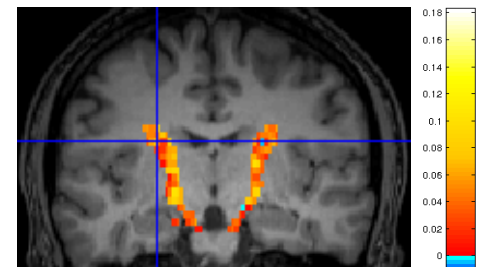


Fig 2. Color-coded map of  $E_{\text{par}} - E_{\text{perp}}$  in the CST, overlaid on a coronal T1-weighted image.